https://doi.org/10.5194/egusphere-2026-4535
Preprint. Discussion started: 31 August 2026

A Physically Self-Consistent Baseline Model and Spatial Distribution Simulation for Global Cosmogenic Nuclide Production Rates

Dingxiong Chen[1], Hongtao Shen[1 2]

[1]College of Physics and Technology, Guangxi Normal University, Guilin, Guangxi 541004, China

[2]Guangxi Key Laboratory of Nuclear Physics and Nuclear Technology, Guilin, Guangxi 541004, China

Correspondence to: Hongtao Shen (shenht@gxnu.edu.cn)

Abstract. This paper develops a numerical model of cosmic-ray interactions with the Earth's atmosphere using the Geant4 Monte Carlo package, and simulates the neutron flux distribution over flat, unshielded terrain at various latitudes and altitudes globally. The production rates of cosmogenic nuclides (^{10}Be, ^{26}Al, ^{14}C, and ^{21}Ne) are calculated using a "baseline production rate + flux scaling factor" strategy: baseline production rates for each nuclide are first obtained by convolving the neutron energy spectrum with experimental excitation functions at a reference point, and then extrapolated globally using the spatial scaling factors of neutron flux derived from Geant4 simulations. The results are systematically compared with the Argento (MCNP) and Lifton (LSDn) models, showing good agreement under most conditions. This work is based on a pure Geant4 framework, with all scaling factors derived from unified physical simulations and without introducing any empirical scaling factors fitted to measured data. It provides a physically self-consistent baseline reference for global-scale calculations of cosmogenic nuclide production rates.

1. Introduction

Cosmic rays interacting with the Earth's atmosphere generate a large number of secondary particles, which in turn produce cosmogenic nuclides such as ^{10}Be, ^{26}Al, ^{14}C, and ^{21}Ne(Schaefer et al., 2022; Gosse and Phillips, 2001; Ivy-Ochs and Kober, 2008; Granger and Muzikar, 2001). These nuclides are widely used in surface exposure dating, burial dating, and reconstruction of geological processes, and the accuracy of production rate calculations directly determines the reliability of dating results. In the development of methodologies, Lal & Peters (1967) first established the physical framework for cosmogenic nuclide production rates (the "Lal–Peters curve"), but their

https://doi.org/10.5194/egusphere-2026-4535
Preprint. Discussion started: 31 August 2026

approach relied on analytical approximations, with precision limited by the computational capabilities of that era. Masarik (1995), based on the LAHET Code System, introduced Monte Carlo methods into this field for the first time, demonstrating the feasibility of numerical simulations, although the code has since become outdated. Gordon et al.(2004) measured ground-level neutron fluxes across the United States using Bonner sphere spectrometers, revealing the spectral structure, but the measurement coverage was limited and difficult to extrapolate globally. Masarik & Beer (2009) employed a hybrid GEANT/MCNP code to investigate the effects of solar activity and the geomagnetic field on production rates, but their approach relied on data exchange between different codes. Dunai (2000) incorporated the non-dipole components of the geomagnetic field into the scaling framework; however, Desilets et al. (2001) pointed out that outdated data were used, and this controversy exposed the inherent limitations of purely empirical scaling methods. Argento (2015) conducted independent simulations based on MCNP6 without code mixing, but its nuclear database (ENDF/B-VII) and transport algorithms exhibit systematic differences from those of Geant4. The LSDn model of Lifton et al. (2014) employs analytical approximations combined with empirical corrections, offering computational simplicity, yet its accuracy is constrained by the applicability of fitting functions in regions with complex geomagnetic fields. Čechvala et al. (2023) validated the feasibility of Geant4 in extraterrestrial scenarios, but did not address the complex environment of Earth's atmosphere. A common issue underlying all the above works is that different models adopt different code combinations, nuclear databases, transport algorithms, or empirical correction factors, making it difficult to establish a unified physical baseline among the results and rendering the physical sources of production rate deviations difficult to trace. To address this gap, our solution is as follows: based on a pure Geant4 framework, we employ a unified physics list (QGSP_BIC_HP) and a single nuclear database (G4NDL) to independently complete the entire workflow, from primary GCR particle emission and atmospheric modeling to neutron flux simulation. Production rates are calculated using a "baseline production rate + flux scaling factor" strategy, with all scaling factors derived from simulations within the same physical framework and without introducing any empirical scaling factors fitted to measured data. This paper calculates the global distributions of production rates for ^{10}Be, ^{26}Al, ^{14}C, and ^{21}Ne in surface rocks, covering all latitudes (0°–90°) and elevations from 0 to 5 km, and systematically compares the results with the

https://doi.org/10.5194/egusphere-2026-4535
Preprint. Discussion started: 31 August 2026

Argento and Lifton (LSDn) models. The spatial distributions of production rates are entirely predicted by a physically self-consistent model, and all results are presented for flat, unshielded surface conditions, providing a clear baseline reference for subsequent studies incorporating shielding effects such as topography and vegetation.

2. Methods for Cosmogenic Nuclide Production Rate Calculation

The development of in situ cosmogenic nuclide production rate calibration methods has undergone an evolution from "purely empirical constraints" to "analytical parameterization," and then to "full physical simulation." Throughout this progression, the underlying tension between computational efficiency and physical fidelity, as well as the issue of physical self-consistency across different Monte Carlo frameworks, has remained persistent.Phase I (1990s–early 2000s): Empirical Calibration and Foundational Analytical FrameworksLal (1991), based on limited global neutron monitor data and a small number of geological calibration sites, proposed a latitude-altitude production rate polynomial under the dipole field approximation(Lal, 1991). The fundamental deficiency of this scheme lies in the fact that neutron monitor stations are predominantly concentrated in the mid-to-high latitudes of the Northern Hemisphere, leaving the polynomial coefficients for the Southern Hemisphere and oceanic regions essentially unconstrained. Stone (2000) improved the mathematical formulation of the polynomial(Stone, 2000), but did not overcome this data scarcity predicament. The defining methodological characteristic of this phase is the "constraint of nuclide production rates by geological calibration sites"—the accuracy of production rates was entirely dependent on the accuracy of geological age constraints, forming an inextricable circular dependency.Phase II (2006–2014): The Advent of Monte Carlo Simulations and Parameterization Refinement.Desilets et al. (2006) recalibrated the non-dipole components within the Lal-Stone framework using Monte Carlo simulations for the first time(Desilets et al., 2006), shifting the anchor point of production rate calibration from geological age constraints partially toward nuclear physics simulations—a significant methodological advancement. However, its limitation lay in the fact that the structure of the analytical expressions remained unchanged; the inherent smoothness of the polynomial merely redistributed rather than eliminated the fitting residuals in regions of strong geomagnetic anomalies. (Webber et al., 2007) (Sato et al., 2008)

https://doi.org/10.5194/egusphere-2026-4535
Preprint. Discussion started: 31 August 2026

using FLUKA and PHITS respectively, independently calculated cosmic-ray neutron energy spectra, yet exposed a deeper issue: due to differences in hadronic interaction models and low-energy neutron cross-section libraries between different Monte Carlo codes, the vertical neutron flux profiles produced exhibited systematic normalization discrepancies. During this period, "code dependency" gradually emerged as an unavoidable methodological issue. The LSDn model of (Lifton et al., 2014) represents the integration of this approach—essentially an analytical approximation of Monte Carlo simulation results with empirical corrections. While computationally efficient, the empirical correction factors depend on specific code versions and geomagnetic field models, making extrapolation uncertainties difficult to quantify when transferring to different geomagnetic reference models.Phase III (2015–present): The Rise of Full Physical Simulation and the Salient Demand for Methodological Self-ConsistencyArgento (2015), based on MCNP6 and the ENDF/B-VII nuclear database(Argento et al., 2015), achieved a transition from functional approximation to particle tracing by calculating geomagnetic cutoff rigidities through particle-by-particle trajectory tracking in a real dipole field. However, its full accuracy is constrained by the fundamental discrepancies in core physical modeling between MCNP and Geant4: at the hadronic physics level, differences in cascade and fragmentation models between the two codes lead to discrepancies in the hardness and angular distribution of secondary neutron spectra; in thermal neutron treatment, MCNP relies on the S(α,β) thermal scattering law from the ENDF/B library, whereas Geant4's HP model features different descriptions of low-energy neutron thermalization details; at the nuclear database level, identifiable deviations exist between ENDF/B-VII and G4NDL for specific nuclide reaction cross-sections. These discrepancies represent systematic deviations under different physical approximation systems. Embedding Argento's production rate coefficients directly into a Geant4 workflow would mean that production rate calibration and target application operate under different physical assumptions, constituting an unresolvable source of error. The broader lesson is general: production rate coefficients are not transferable across codes; calibration and application must be conducted within a strictly unified physical framework.

Based on the above examination of methodological deficiencies across the three technical phases—the circular dependency of empirical calibration, the structural limitations of

https://doi.org/10.5194/egusphere-2026-4535
Preprint. Discussion started: 31 August 2026

parameterization schemes, and the risk of physical inconsistency in cross-code transfer—this study adopts a pure Geant4-based production rate calibration strategy. All scaling coefficients are derived from a single physics list (QGSP_BIC_HP) and a single nuclear database (G4NDL), with no empirical correction factors introduced, ensuring physical self-consistency throughout the entire logical chain from cosmic-ray incidence to nuclide accumulation. The High Precision (HP) neutron model within QGSP_BIC_HP directly affects the production rate accuracy of nuclides such as ^{10}Be through its treatment of thermal neutron capture reactions—precisely the critical area where disagreements between different codes emerge. This work aims to establish a physically pristine, traceable benchmark calibration system.

3. Production Rate Calculation Strategy: Benchmark Production Rate and Flux Scaling

This paper proposes an equivalent scheme of "benchmark production rate + flux scaling coefficients." The core innovation of this scheme lies in concentrating the physical rigor of production rate calibration at a single reference point, while reducing the simulation of spatial distribution to a pure neutron transport problem, thereby achieving an optimal balance between physical self-consistency and computational feasibility. The physical basis for this approach is that the production of cosmogenic nuclides (e.g., ^{10}Be, ^{14}C) is predominantly governed by fast-neutron spallation reactions, with excitation functions varying relatively smoothly over a broad energy range (~10 MeV to several GeV), making the effect of variations in neutron spectral shape with geographical location on the production rate scaling ratio only a secondary effect. This characteristic is the physical prerequisite for the validity of the present scheme and constitutes its fundamental distinction from previous empirical scaling methods—the scaling coefficients are entirely determined by Geant4 hadron transport physics, with no empirical correction factors introduced, thereby preserving the same physical kernel as the reference point.

The implementation proceeds in three steps. (1) Rigorous calibration of the benchmark production rate: A reference point at low latitude (0°–10°) and an altitude of 5 km is selected, where geomagnetic shielding is weakest and the fast-neutron flux fraction is maximized, effectively suppressing interference from the thermal neutron capture component. The complete neutron differential energy spectrum $\Phi_{ref}(E)$ is simulated at this point and rigorously convolved with the

https://doi.org/10.5194/egusphere-2026-4535
Preprint. Discussion started: 31 August 2026

experimentally constrained excitation functions $\sigma_i(E)$ on an energy-point-by-energy-point basis to obtain the benchmark absolute production rate P_{ref} for each nuclide (see Table 3). This convolution is the sole complete spectrum–cross-section coupled calculation in the scheme, and its accuracy directly determines the absolute accuracy of the entire production rate calibration system. (2) Physical transport simulation of spatial scaling coefficients: For all latitude/altitude grid points, the neutron flux ratio relative to the reference point is independently simulated to obtain the scaling coefficients $S(\lambda,h)$ (see Table 2). These coefficients are derived directly from Geant4 simulations of the complete atmospheric cascade process of primary cosmic-ray particles, with geomagnetic cutoff rigidity deflection and the modulation of secondary neutron energy spectra by atmospheric depth both described uniformly by the same physics list (QGSP_BIC_HP) and nuclear database (G4NDL), ensuring complete physical self-consistency with the reference point. (3) The final production rate is given by $P(\lambda,h) = P_{ref} \times S(\lambda,h)$.

This scheme offers three advantages over existing approaches. First, physical self-consistency: The entire logical chain from cosmic-ray incidence to nuclide accumulation is closed within the same Geant4 physical framework, fundamentally avoiding the risk of physical inconsistency caused by cross-code transfer between production rate calibration and target application that plagued previous studies. Second, computational efficiency and traceability: The costly point-by-point convolution is reduced to a single accurate benchmark convolution plus a series of pure transport simulations, achieving an order-of-magnitude improvement in efficiency. Moreover, the origin of each production rate value can be traced back to specific physical processes, without the information loss caused by polynomial smoothing in parameterization schemes. Third, extensibility: This framework physically decouples absolute production rate calibration from spatial distribution simulation—if more accurate excitation function experimental data become available in the future, only the reference point P_{ref} needs to be updated, and the global grid can be directly mapped using the existing scaling coefficients without the need for repeated large-scale particle transport simulations. This capability is not possessed by any parameterization or empirical calibration scheme.

3.1 Composition of Galactic Cosmic Rays

https://doi.org/10.5194/egusphere-2026-4535
Preprint. Discussion started: 31 August 2026

Galactic cosmic rays (GCR) are composed of 87% protons, 12% alpha particles, and 1% heavy nuclei [19]. In this study, the solar modulation potential φ is set to 550 MV, which governs the spectral shape of the GCR differential energy spectrum—higher φ values indicate stronger solar activity and correspondingly lower GCR fluxes. The simulation employs the Geant4 General Particle Source (GPS) module, with a spherical shell of radius 6478 km centered at the Earth's center as the emission source. Particles are generated uniformly on the spherical surface, with emission directions following a local cosine-law angular distribution. A total of 5×10^6 primary particles are emitted. The omnidirectional flux of GCR protons is 3.18 $cm^{-2}\ s^{-1}$, and that of alpha particles is 0.22 $cm^{-2}\ s^{-1}$(Chen et al., 2017). It should be particularly noted that these values represent the 4π integrated flux, i.e., the total particle emission rate per unit area of the spherical shell surface into all outward directions. In the actual physical scenario, any point on the spherical shell surface only receives incident particles from the upper hemisphere; the effective flux must be integrated over the zenith angle θ (from 0 to π/2) and azimuthal angle ϕ,as shown in **Eq. (1)**

$$I_{\text{eff}} = I_0 \int_0^{2\pi} d\,\phi \int_0^{\frac{\pi}{2}} \cos\theta \sin\theta d\theta = I_0 \cdot 2\pi \cdot \frac{1}{2} = \pi I_0 \qquad (1)$$

where θ is the angle between the particle incidence direction and the surface normal (zenith angle), and ϕ is the azimuthal angle. Since the 4π integrated flux is $I_0 \times 4\pi$, the ratio of the effective surface flux to this value is given by **Eq. (2)**

$$\frac{I_{\text{eff}}}{I_0 \times 4\pi} = \frac{\pi I_0}{4\pi I_0} = \frac{1}{4} \qquad (2)$$

Therefore, the effective flux should be one-quarter of the shell emission flux, i.e. 0.795 $cm^{-2} \cdot s^{-1}$. This treatment accurately reflects the actual physical scenario of GCR particles interacting with the planetary surface, ensuring the subsequent correctness of cosmogenic nuclide production rate calculations.

3.2 Geophysical Models

3.2.1 Earth's External Magnetic Field

J. Masarik and J. Beer designed the geomagnetic field based on particle magnetic rigidity (momentum per unit charge, R = pc/Ze, where p is momentum, Ze is the particle charge, and c is

https://doi.org/10.5194/egusphere-2026-4535
Preprint. Discussion started: 31 August 2026

the speed of light) [6], and converged the vertical cutoff rigidity at every 10° latitude. In this study, the cutoff rigidity of the Earth's magnetic field is calculated using the formula $Rc = 14.9 \times \cos^4(\lambda)$, where λ denotes the geomagnetic latitude. This formula reflects the characteristic that cutoff rigidity increases with increasing latitude, reaching its minimum near the polar regions (λ = 90°) and its maximum at the equator (λ = 0°). It should be noted that this magnetic field expression is only an approximation, which may introduce deviations in the calculated flux and production rates. It is also worth pointing out that this dipole field approximation introduces certain deviations in low-latitude regions, particularly over the South Atlantic Anomaly. Nevertheless, for a global-scale benchmark simulation, the balance between computational efficiency and physical simplicity is reasonable.

3.2.2 Earth's Composition and Structure

In the simulations presented herein, the Earth is approximated as a uniform sphere with a radius of 6378 km and a surface density of 2 g/cm³ (with elemental composition and proportions listed in Table 1). The Earth's atmosphere is modeled as a spherical shell of 100 km thickness, further subdivided into 60 concentric layers: the first 50 layers each with a thickness of 1 km, and the remaining 10 layers each with a thickness of 5 km. The average chemical composition of the atmosphere in each layer adopts an approximate ratio (N: 75.5%, O: 23.2%, Ar: 1.3%), while the vertical distribution of atmospheric density and temperature follows the 1976 U.S. Standard Atmosphere model(Coesa, 1976), thereby ensuring the realism and reliability of the simulations.

Table 1 Composition and proportions of elements on the Earth's surface

Element	**Soil**
H	0.002
O	0.473
Na	0.025
Mg	0.040
Al	0.060
Si	0.290
Ca	0.050
Fe	0.060

https://doi.org/10.5194/egusphere-2026-4535
Preprint. Discussion started: 31 August 2026

3.2.3 Physics Interaction Models

In this study, the QGSP_BIC_HP physics list in Geant4 is selected as the collection of physical processes for simulation. This physics list is specifically designed for hadronic interactions and high-precision neutron physics, making it highly suitable for simulation studies of cosmic-ray interactions with atmospheric and surface materials. The QGSP_BIC_HP physics list encompasses electromagnetic interactions, strong interactions, high-precision neutron physics (HP), nuclear reaction processes, decay processes, and others. The production rate of cosmogenic nuclides can be calculated using the following expression(Leya et al., 2000): as shown in **Eq. (3)**

$$P_i = \sum_k \sum_j N_j \int J_k(E,d)\sigma_{i,k}(E)\, dE \qquad (3)$$

where N_j is the concentration of target element j in the material, $J_k(E,d)$ is the differential flux of particle type k at depth d below the material surface, and $\sigma_{i,k}^{j}(E)$ is the excitation function for the interaction of particle type k with target element j at energy E, producing nuclide i.

4. Results

Based on Geant4 simulations, this study obtained the neutron flux scaling coefficients for different latitudes and altitudes (Table 2).

Table 2 Neutron flux scaling coefficients at different latitudes and altitudes based on Geant4 simulations

altitude / latitude	0 km	1 km	2 km	3 km	4 km	5 km
0°-10°	0.43	0.87	1.68	2.93	4.85	7.23
10°-20°	0.47	0.96	1.87	3.33	5.49	8.31
20°-30°	0.52	1.11	2.15	3.93	6.67	10.35
30°-40°	0.68	1.49	2.99	5.62	9.61	15.28
40°-50°	0.87	2.02	4.16	7.98	14.24	23.05
50°-60°	0.94	2.26	4.87	9.54	17.27	29.31
60°-70°	1	2.32	4.88	9.74	17.77	30.07
70°-90°	1	2.24	4.81	9.39	17.59	29.83

https://doi.org/10.5194/egusphere-2026-4535
Preprint. Discussion started: 31 August 2026

Based on Equation (3), the production rates of ^{10}Be, ^{26}Al, ^{14}C, and ^{21}Ne in silica (SiO_2) at an altitude of 5 km in the reference region (0°–10° latitude) were calculated [units: atoms/(g·year)]. The results are presented in Table 3.

Table 3 Cosmogenic nuclide production rates in the low-latitude (0°–10°) region at 5 km altitude [atoms/(g·year)]

	This work	Target
^{10}Be	40.2	SiO_2
^{26}Al	271.6	SiO_2
^{21}Ne	156.8	SiO_2
^{14}C	122.5	SiO_2

Based on the neutron flux scaling coefficients obtained from Geant4 simulations in Table 3, the spatial distributions of the production rates for the aforementioned nuclides in each region were further derived. The results are presented in Figures 1 through 4, respectively.

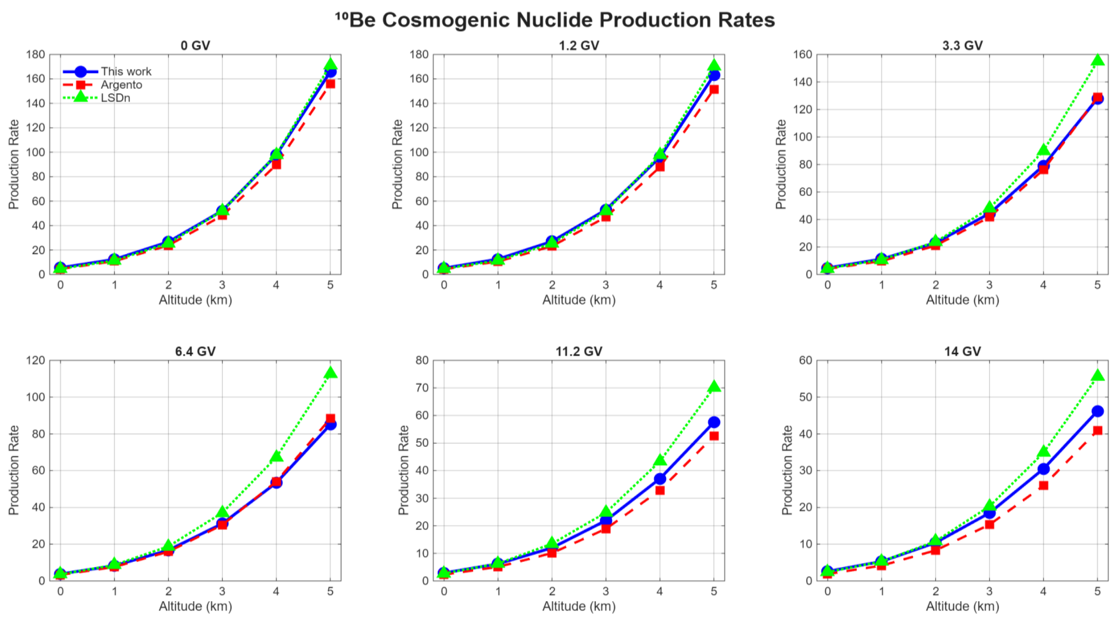

Fig. 1 ^{10}Be production rate versus altitude under different cutoff rigidities.

https://doi.org/10.5194/egusphere-2026-4535
Preprint. Discussion started: 31 August 2026

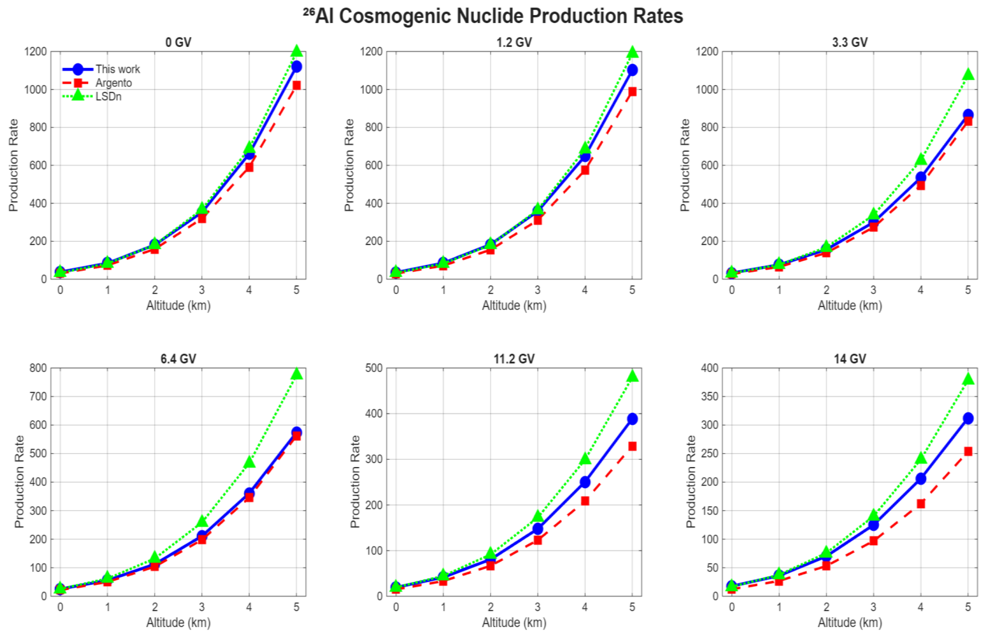

Fig. 2 ^{26}Al production rate versus altitude under different cutoff rigidities.

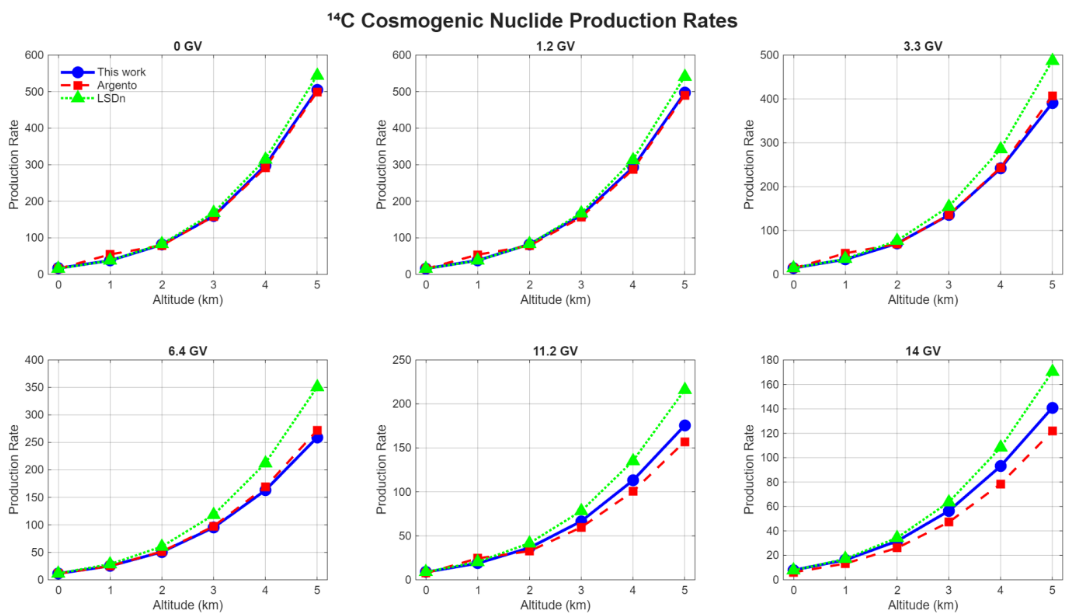

Fig. 3 ^{14}C production rate versus altitude under different cutoff rigidities.

https://doi.org/10.5194/egusphere-2026-4535
Preprint. Discussion started: 31 August 2026

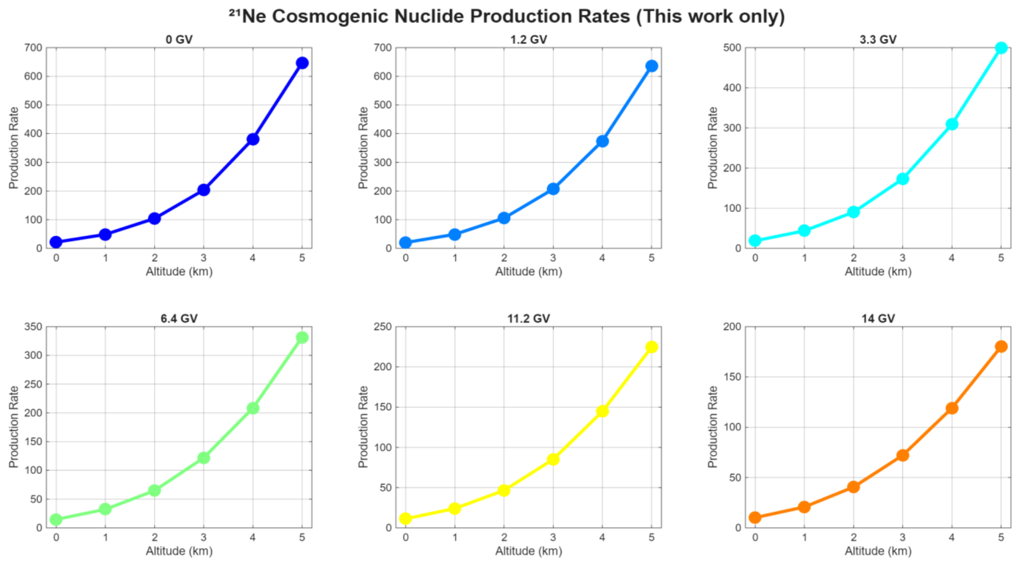

Fig. 4 ^{21}Ne production rate versus altitude under different cutoff rigidities

A systematic comparison was conducted between the results of this work and those of Argento (MCNP-based simulation) and the LSDn model (see Tables S1–S4). For ^{10}Be and ^{26}Al, the values calculated in this work fall, under the vast majority of conditions, between the Argento and LSDn results, exhibiting an "intermediate" characteristic. At low altitudes (0–2 km), the results are in excellent agreement with LSDn (within ±5% deviation), while at mid-to-high altitudes (3–5 km), the discrepancies increase systematically. The physical origin of this lies in the fact that at high altitudes, the thinner atmosphere leads to a sharp increase in the proportion of high-energy secondary particles, amplifying the fundamental differences among models in nuclear databases and transport algorithms. In terms of latitudinal gradients, all three models converge at low cutoff rigidities (polar regions), while discrepancies are amplified at high cutoff rigidities (equatorial regions). Furthermore, ^{26}Al exhibits a larger dispersion than ^{10}Be due to its greater sensitivity to spectral shape. For ^{14}C, the results show excellent consistency with LSDn at low altitudes and in polar regions. However, systematic deviations appear at mid-to-high altitudes under intermediate cutoff rigidities, where the values are even lower than both reference models. This is attributed to the particular dependence of ^{14}C on thermal neutron capture reactions, where the differences between Geant4's HP neutron transport module and MCNP in thermal neutron cross-sections and

https://doi.org/10.5194/egusphere-2026-4535
Preprint. Discussion started: 31 August 2026

moderation treatments are further amplified under the complex geomagnetic field configurations at intermediate latitudes. This deviation precisely exposes the systematic differences among different code schemes in the thermal neutron energy region, and the pure Geant4 framework of this work provides a self-consistent reference system for identifying this issue. For the stable nuclide ^{21}Ne, the production rate exhibits a slow increase at low altitudes and a steeper increase at high altitudes with rising elevation, and increases monotonically with decreasing cutoff rigidity. Its spatial distribution pattern is physically self-consistent with cosmic-ray transport physics, providing benchmark parameters for relevant geological applications.

5. Discussion and Conclusion

In this study, a numerical model of cosmic-ray interactions with the Earth's atmosphere was established within the Geant4 framework. The neutron flux distribution at various latitudes and altitudes was systematically simulated on a global scale, and the production rates of key cosmogenic nuclides—^{10}Be, ^{26}Al, ^{14}C, and ^{21}Ne—were calculated using the "benchmark production rate + flux scaling coefficient" strategy. Under a Galactic cosmic-ray modulation potential of 550 MV, the calculated production rates for all nuclides are in good agreement with the Argento (MCNP) and Lifton (LSDn) models under most conditions. All scaling coefficients for the spatial distribution of production rates are derived from unified Geant4 physical simulations, without introducing any empirical correction factors based on fits to measured data. The discussion of results indicates that, although the overall consistency with existing models validates the effectiveness of the present scheme, there remain systematic biases that could be further optimized. The simplified geomagnetic model ($R_c = 14.9 \cos^4\lambda$), while computationally feasible, neglects the non-dipole components and regional anomalies of the actual geomagnetic field (such as the South Atlantic Anomaly), potentially introducing local production rate biases at low latitudes. Future work could incorporate higher-order models such as the International Geomagnetic Reference Field (IGRF) to improve the accuracy of geomagnetic cutoff rigidity calculations.From the analytical estimations of Lal & Peters (1967), to the LCS numerical simulations of Masarik (1995), the GEANT/MCNP hybrid scheme of Masarik & Beer (2009), the MCNP6 simulations of Argento (2015), and the LSDn empirical correction model of Lifton (2014), existing methods have relied,

https://doi.org/10.5194/egusphere-2026-4535
Preprint. Discussion started: 31 August 2026

to varying degrees, on analytical approximations, cross-code data exchange, switching between external nuclear databases, or empirical data-fitting corrections. The present work, under a pure Geant4 framework with a single physics list (QGSP_BIC_HP), a single nuclear database (G4NDL), and a unified particle emission geometry, independently completes the entire workflow from GCR incidence to global spatial distribution of production rates in a self-contained benchmark simulation. This methodological advantage positions the results of this work as a physical reference baseline for subsequent hybrid schemes and empirical model calibrations.

In summary, the main contribution of this study is the development of a physically self-consistent and computationally efficient simulation framework. This framework innovatively combines a spherical-shell particle source with a flux scaling strategy, enabling global predictions of multi-nuclide production rates while maintaining computational efficiency. Although there remains room for improvement in low-energy neutron simulations and geomagnetic modeling, the overall model performance is robust, providing a reliable theoretical foundation and computational tool for cosmogenic nuclide dating techniques, particularly suitable for regions lacking empirical calibration data. Future work could further enhance the model's prediction accuracy in geomagnetically anomalous regions by incorporating more refined physical models and more realistic geomagnetic field data.

Code and data availability

The Geant4 simulation code and the cosmogenic nuclide production rate datasets generated in this study have been deposited in an open-access repository and are freely available at https://doi.org/10.5281/zenodo.18653593 (Chen, 2026). The data are publicly accessible and no restrictions apply.

https://doi.org/10.5194/egusphere-2026-4535
Preprint. Discussion started: 31 August 2026

Author contributions

Dingxiong Chen, Hongtao Shen ,conceptualized the study, designed the model framework, and led the writing. All authors contributed to the interpretation of results and editing of the manuscript.

Competing interests

The authors declare that they have no conflict of interest.

Disclaimer

Copernicus Publications remains neutral with regard to jurisdictional claims made in the text, published maps, institutional affiliations, or any other geographical representation in this paper. While Copernicus Publications makes every effort to include appropriate place names, the final responsibility lies with the authors. Views expressed in the text are those of the authors and do not necessarily reflect the views of the publisher.

Acknowledgements

This work was supported by the Central Government Guidance Funds for Local Scientific and Technological Development, China (No. Guide ZY22096024), the National Natural Science Foundation of China (Nos. 11775057 and 11765004), and JSPS KAKENHI under Grant No. 23K23269.

Financial support

This research has been supported by the Central Government Guidance Funds for Local Scientific and Technological Development, China (grant no. Guide ZY22096024), the National Natural Science Foundation of China (grant nos. 11775057 and 11765004), and the Japan Society for the Promotion of Science (grant no. 23K23269).

https://doi.org/10.5194/egusphere-2026-4535
Preprint. Discussion started: 31 August 2026

References

Argento, D. C., Stone, J. O., Reedy, R. C., and O'Brien, K.: Physics-based modeling of cosmogenic nuclides part II -- Key aspects of in-situ cosmogenic nuclide production, Quat. Geochronol., 26, 44--55, https://doi.org/10.1016/j.quageo.2014.09.005, 2015.

Čechvala, P., Breier, R., and Masarik, J.: Production rates of cosmogenic nuclides in extraterrestrial material using GEANT4 software, J. Radioanal. Nucl. Chem., 332, 4403--4411, https://doi.org/10.1007/s10967-023-08954-0, 2023.

Chen, J., Dong, T., and Ren, Z.: Calibrating a physical model based on Geant4 to calculate cosmogenic nuclide production rates on lunar surface, Meteorit. Planet. Sci., 52, 646--655, https://doi.org/10.1111/maps.12812, 2017.

Coesa, U. S.: Standard atmosphere, 1976, US Government Printing Office, Washington, DC, 1976.

Desilets, D., Zreda, M., and Lifton, N. A.: Comment on "Scaling factors for production rates of in situ produced cosmogenic nuclides: a critical reevaluation" by Tibor J. Dunai, Earth Planet. Sc. Lett., 188, 283--287, https://doi.org/10.1016/S0012-821X(01)00320-8, 2001.

Desilets, D., Zreda, M., and Prabu, T.: Extended scaling factors for in situ cosmogenic nuclides: new measurements at low latitude, Earth Planet. Sc. Lett., 246, 265--276, https://doi.org/10.1016/j.epsl.2006.03.051, 2006.

Dunai, T. J.: Scaling factors for production rates of in situ produced cosmogenic nuclides: a critical reevaluation, Earth Planet. Sc. Lett., 176, 157--169, https://doi.org/10.1016/S0012-821X(99)00310-0, 2000.

Gordon, M. S., Goldhagen, P. E., Rodbell, K. P., Zabel, T. H., Tang, H. H. K., Clem, J. M., and Bailey, P.: Measurement of the flux and energy spectrum of cosmic-ray induced neutrons on the ground, IEEE Trans. Nucl. Sci., 51, 3427-3434, https://doi.org/10.1109/TNS.2004.839134, 2004.

Gosse, J. C. and Phillips, F. M.: Terrestrial in situ cosmogenic nuclides: theory and application, Quaternary Sci. Rev., 20, 1475--1560, https://doi.org/10.1016/S0277-3791(00)00171-2, 2001.

https://doi.org/10.5194/egusphere-2026-4535
Preprint. Discussion started: 31 August 2026

Granger, D. E. and Muzikar, P. F.: Dating sediment burial with in situ-produced cosmogenic nuclides: theory, techniques, and limitations, Earth Planet. Sc. Lett., 188, 269--281, https://doi.org/10.1016/S0012-821X(01)00309-9, 2001.

Ivy-Ochs, S. and Kober, F.: Surface exposure dating with cosmogenic nuclides, E&G Quaternary Sci. J., 57, 179--209, https://doi.org/10.3285/eg.57.1-2.7, 2008.

Lal, D.: Cosmic ray labeling of erosion surfaces: in situ nuclide production rates and erosion models, Earth Planet. Sc. Lett., 104, 424--439, https://doi.org/10.1016/0012-821X(91)90220-C, 1991.

Lal, D. and Peters, B.: Cosmic ray produced radioactivity on the Earth, in: Kosmische Strahlung II/Cosmic Rays II, edited by: Sitte, K., Springer, Berlin, 551--612, https://doi.org/10.1007/978-3-642-46079-1_7, 1967.

Leya, I., Lange, H.-J., Neumann, S., Wieler, R., and Michel, R.: The production of cosmogenic nuclides in stony meteoroids by galactic cosmic-ray particles, Meteorit. Planet. Sci., 35, 259--286, https://doi.org/10.1111/j.1945-5100.2000.tb01777.x, 2000.

Lifton, N., Sato, T., and Dunai, T. J.: Scaling in situ cosmogenic nuclide production rates using analytical approximations to atmospheric cosmic-ray fluxes, Earth Planet. Sc. Lett., 386, 149--160, https://doi.org/10.1016/j.epsl.2013.10.052, 2014.

Masarik, J. and Beer, J.: An updated simulation of particle fluxes and cosmogenic nuclide production in the Earth's atmosphere, J. Geophys. Res.-Atmos., 114, D11103, https://doi.org/10.1029/2008JD010557, 2009.

Masarik, J. and Reedy, R. C.: Terrestrial cosmogenic-nuclide production systematics calculated from numerical simulations, Earth Planet. Sc. Lett., 136, 381--395, https://doi.org/10.1016/0012-821X(95)00169-D, 1995.

Sato, T., Yasuda, H., Niita, K., Endo, A., and Sihver, L.: Development of PARMA: PHITS-based analytical radiation model in the atmosphere, Radiat. Res., 170, 244--259, https://doi.org/10.1667/RR1094.1, 2008.

Schaefer, J. M., Codilean, A. T., Willenbring, J. K., et al.: Cosmogenic nuclide techniques, Nat. Rev. Methods Primers, 2, 18, https://doi.org/10.1038/s43586-022-00096-9, 2022.

https://doi.org/10.5194/egusphere-2026-4535
Preprint. Discussion started: 31 August 2026

Simpson, J. A.: Elemental and isotopic composition of the galactic cosmic rays, Ann. Rev. Nucl. Part. Sci., 33, 323--382, https://doi.org/10.1146/annurev.ns.33.120183.001543, 1983.

Stone, J. O.: Air pressure and cosmogenic isotope production, J. Geophys. Res.-Solid, 105, 23753--23759, https://doi.org/10.1029/2000JB900181, 2000.

Webber, W. R., Higbie, P. R., and McCracken, K. G.: Production of the cosmogenic isotopes ^{3}H, ^{7}Be, ^{10}Be, and ^{36}Cl in the Earth's atmosphere by solar and galactic cosmic rays, J. Geophys. Res.-Space, 112, A10106, https://doi.org/10.1029/2007JA012499, 2007.